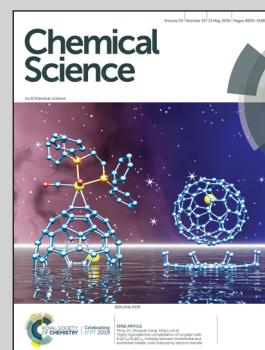


Showcasing research from Professor Zigang Li's laboratory,
School of Chemistry, Peking University, Shenzhen, China.

A sulfonium tethered peptide ligand rapidly and selectively
modifies protein cysteine in vicinity

Herein, we report a unique peptide macrocyclization method *via* the bis-alkylation between methionine and cysteine to generate cyclic peptides with significantly enhanced stability and cellular uptake. Notably, when the cyclized peptide ligand selectively recognizes its protein target with a proximate cysteine, a rapid nucleophilic substitution could occur between the protein Cys and the sulfonium center on the peptide to form the conjugate. The conjugation reaction is rapid, facile and selective, triggered solely by proximity. This method shows great potential for protein profiling, cell imaging and antibody–drug conjugates.

As featured in:



See Shuiming Li,
Feng Yin, Zigang Li *et al.*,
Chem. Sci., 2019, **10**, 4966.

Cite this: *Chem. Sci.*, 2019, 10, 4966

All publication charges for this article have been paid for by the Royal Society of Chemistry

A sulfonium tethered peptide ligand rapidly and selectively modifies protein cysteine in vicinity[†]

Dongyuan Wang,^{‡a} Mengying Yu,^{‡a} Na Liu,^a Chenshan Lian,^a Zhanfeng Hou,^a Rui Wang,^b Rongtong Zhao,^a Wenjun Li,^a Yixiang Jiang,^a Xiaodong Shi,^a Shuiming Li,^{*c} Feng Yin^{id}^{*a} and Zigang Li^{id}^{*a}

Significant efforts have been invested to develop site-specific protein modification methodologies in the past two decades. In most cases, a reactive moiety was installed onto ligands with the sole purpose of reacting with specific residues in proteins. Herein, we report a unique peptide macrocyclization method *via* the bis-alkylation between methionine and cysteine to generate cyclic peptides with significantly enhanced stability and cellular uptake. Notably, when the cyclized peptide ligand selectively recognizes its protein target with a proximate cysteine, a rapid nucleophilic substitution could occur between the protein Cys and the sulfonium center on the peptide to form a conjugate. The conjugation reaction is rapid, facile and selective, triggered solely by proximity. The high target specificity is further proved in cell lysate and hints at its further application in activity based protein profiling. This method enhances the peptide's biophysical properties and generates a selective ligand-directed reactive site for protein modification and fulfills multiple purposes by one modification. This proof-of-concept study reveals its potential for further broad biological applications.

Received 3rd January 2019

Accepted 24th March 2019

DOI: 10.1039/c9sc00034h

rsc.li/chemical-science

Introduction

Site selective protein conjugation provides a controllable tool to directly and precisely analyze protein functions in important cellular processes.¹ Thus, multiple approaches have been developed to selectively modify endogenously reactive amino acid residues in proteins.^{2–5} Chemo-selective reactions on particular residues in proteins are broadly utilized, including cysteine,^{6–9} lysine,^{10–15} tyrosine,¹⁶ tryptophan,¹⁷ arginine¹⁸ and methionine.^{19,20} The development of chemical tools for site-selective protein labeling is in high demand due to its high precision and versatility. These tools include the genetic incorporation of unnatural amino acids within proteins equipped with “bioorthogonal” reactivity,^{21,22} genetic incorporation of peptide sequences (tag) for spatial recognition²³ and the utilization of N-terminal/C-terminal sites for protein labeling.²⁴

Another alternative approach for achieving regio-selectivity is the ligand-induced protein conjugation which is mainly based on a precise spatial positioning between a functional group of a ligand and a reactive residue in protein. Meares *et al.* pioneered this concept in developing antibody conjugation with infinite affinity.²⁵ Recently, Hamachi *et al.* established ligand-directed (LD) chemistry to specifically label a protein of interest (POI) in living cells.^{26,27} Howarth *et al.* reported the Spytag-Spycatcher system in which the 13-residue Spytag peptide spontaneously and selectively forms an isopeptide bond with the Spycatcher-tagged proteins.²⁸ These ligand-directed approaches provide promising opportunities to balance the reactivity and selectivity for protein modification.

Regarding the selection of amino acid residues for ligand-induced protein conjugation, the high nucleophilicity and low abundance of cysteine in proteins make it a prime residue for selective protein conjugation. In general, cysteine residues were allowed to (i) react with electrophilic moieties such as haloalkyl or alkenyl groups; (ii) undergo metal assisted reactions and (iii) be converted into dehydroalanine for further modifications. The diverse methods for selective protein labeling have been widely used in the study of post-translational modifications (PTMs), cellular imaging, activity based protein profiling (ABPP) or covalent drug discovery.^{2,29–31} Notably, covalent inhibitors of key kinases, such as ibrutinib and rociletinib, were recently approved by the FDA as efficient cancer therapeutics.^{32–34}

Peptides have been recently utilized as promising ligands for covalent protein modification due to their high binding

^aState Key Laboratory of Chemical Oncogenomics, School of Chemical Biology and Biotechnology, Peking University Shenzhen Graduate School, Shenzhen, 518055, China. E-mail: lizg@pkusz.edu.cn; yinfeng@pkusz.edu.cn

^bDepartment of Biomedical Sciences, City University of Hong Kong, Kowloon, Hong Kong. E-mail: rwang46@cityu.edu.hk

^cCollege of Life Sciences and Oceanography, Shenzhen University, Shenzhen, 518055, China. E-mail: shuimingli@szu.edu.cn

[†] Electronic supplementary information (ESI) available: Experimental procedures, supporting tables and figures. See DOI: 10.1039/c9sc00034h

[‡] These authors contributed equally to this work.



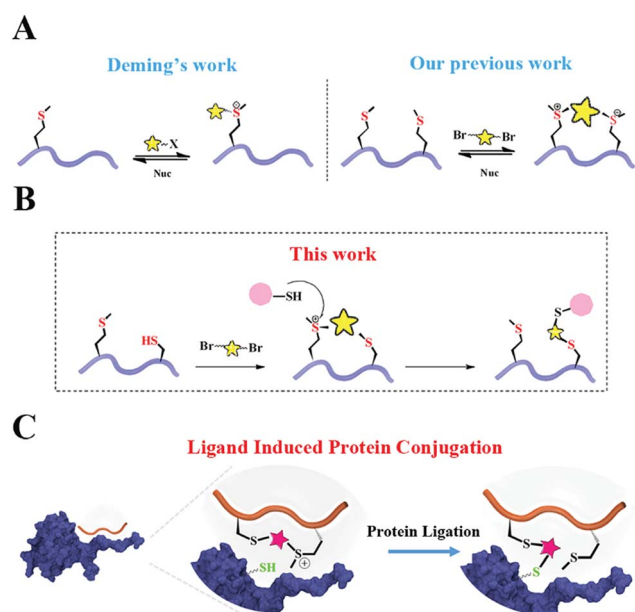
affinity, selectivity and biocompatibility. For example, Xia *et al.* installed a mildly electrophilic α -chloroacetyl moiety onto peptide ligands for covalent conjugation with cysteine near protein–peptide interaction sites.³⁵ Walensky and Fairlie *et al.* independently developed covalent BFL-1 inhibiting stapled peptides with an additional electrophilic warhead acrylamide.^{36–38} Wang *et al.* incorporated aryl sulfonyl fluoride (Ar-SO₂F) in the SAHp53-8 peptide which interrupted p53–Mdm2/4 interactions.³⁹ To the best of our knowledge, all reported methods require a pre-arranged reactive moiety solely for the purpose of conjugation. However, the reactive group either requires special steps to prepare it or may undergo non-specific reactions. For peptides such as the BFL-1 ligands, an additional stapling step is also necessary for enhanced stability and cellular uptake. Thus, we are seeking to develop a facile peptide cyclization method which could enhance the peptides' stability and cellular uptake, meanwhile the modification also generates a highly selective reaction site for reactive amino acid residues in protein.

Based on Deming's pioneering work of selective methionine alkylation, we recently developed a bisalkylation modification of Met to generate cyclic peptides with better cellular uptake and stability.^{40,41} Taking the current protein labelling demands into consideration, we envisioned that this method could be further developed into a novel and facile methodology to fulfil the multiple purposes mentioned above. As shown in Scheme 1, the bis-alkylation between Cys and Met could generate a cyclic peptide with a tuneable tether and an on-tether sulfonium center, which could help in improving the peptide's stability and cellular uptake. The labile sulfonium center may further

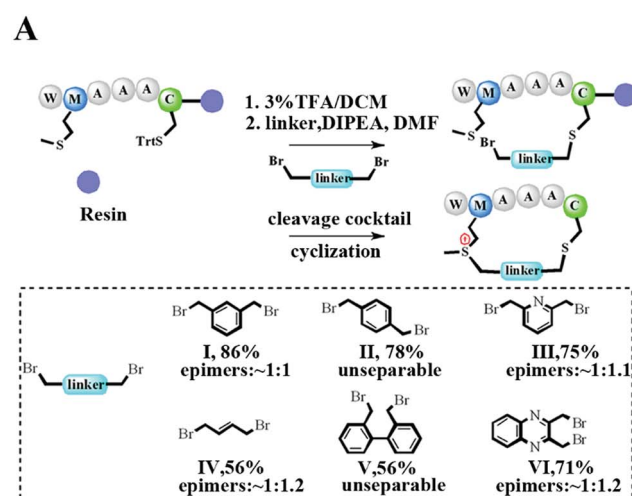
undergo proximity promoted Cys substitution with the available Cys in the vicinity of the POI's binding pocket. Based on previous reports and our own findings, the sulfonium centers are stable in the presence of thiols for a reasonable time, indicating their potential cellular application.^{20,42}

Results and discussion

To meet the demands for both peptide stapling and protein modification, we first used a model hexapeptide (1) to assess the efficiency of peptide cyclization as shown in Fig. 1A. The peptides were constructed *via* conventional Fmoc-based solid phase peptide synthesis. The cyclization involved two steps: (1) the deprotection of Trt-protected cysteine and alkylation with di-halogenated linkers on resin; and (2) the cleavage of the peptide from the resin to give the resulting bis-alkylated cyclic peptides. The alkylation of Met occurred spontaneously



Scheme 1 Schematic representation of Cys–Met bis-alkylation and proximity-promoted protein labeling with a sulfonium tethered peptide. (A) Deming *et al.*'s report of selective methionine alkylation and our previous report of chemoselective methionine bis-alkylation. (B) Peptide macrocyclization through cysteine and methionine bis-alkylation. (C) Ligand induced protein conjugation using the Cys–Met macrocyclization method.



B

Entry	Linear peptide	Linker	Conversion (%)	Epimer ratio (a/b)
1-I	Ac-WMAAAC-NH ₂	I	86	~1:1
2-I	Ac-CAAAM-NH ₂	I	63	unseparable
3-I	Ac-MAEAC-NH ₂	I	83	~1:1
4-I	Ac-MAKAC-NH ₂	I	66	unseparable
5-I	Ac-MAQAC-NH ₂	I	69	unseparable
6-I	Ac-MADAC-NH ₂	I	72	unseparable
7-I	Ac-MATAC-NH ₂	I	78	~1:1
8-I	Ac-MANAC-NH ₂	I	63	unseparable
9-I	Ac-MSERC-NH ₂	I	53	~1:1
10-I	Ac-MWYHC-NH ₂	I	43	~1:1

Fig. 1 Facile construction of stabilized peptides by bisalkylation between Cys and Met. (A) Constrained peptide preparation and different linkers tested in this study. The Trt-protected cysteine was deprotected with 3%TFA in DCM until the yellow colour was no longer present. Then a di-halogenated linker (2.0 equiv.) was added with DIPEA (4.0 equiv.) in DMF and was left to react for 3 hours. Methionine alkylation and peptide cyclization were completed when the resin was cleaved in a TFA mixture (TFA : TIS : H₂O = 95 : 2.5 : 2.5). The epimer ratio was calculated according to the HPLC traces. (B) Ten different peptides were tested for functional residue tolerance.



during resin cleavage to generate the cyclic peptide 1-I with an 86% conversion based on HPLC integration. The formation of the cyclization product was further supported by LC-MS and $^1\text{H-NMR}$ with a clear shift of the phenyl proton shown in Fig. S1.† We further confirmed that the cyclization process occurred during the resin cleavage step instead of the DIPE/DMF step shown in Fig. S2.† Notably, as the Met alkylation will generate a new on-tether chiral center, we successfully isolated two epimers as indicated in Fig. S3.† Then we tested the reaction efficiency of different di-alkylating linkers and found that the peptide (1) reacted smoothly with different linkers to provide products with high conversions as indicated in Fig. 1A and S3.† The epimer ratios of different linkers were generally $\sim 1 : 1$ and in some cases, the peptide epimers were not separable under our HPLC conditions (Fig. S3.†). Notably, the sulfonium chiral center of the purified epimer is not very stable and would slowly racemize into the initial epimer mixtures. In addition, the separable epimers showed similar secondary structures in CD spectroscopy measurements, suggesting that the chiral center had a limited effect on the peptide's secondary structure (Fig. S4.†). To assess the functional group tolerance of our method, ten peptides with different sequences were prepared as summarized in Fig. 1B. All peptides efficiently generated the corresponding cyclic peptides with high conversion rates.

The Met alkylation was reported to be reversible in the presence of appropriate reductants under mild conditions (pH 7.4 PBS, 37°C).⁴⁰ Among the reductants and nucleophiles tested in previous studies, GSH was reported to be the least reactive.⁴⁰ We first tested the reaction rate of sulfonium tethered peptide 1-Ia (1 mM) with 2-mercaptopyridine (10 mM) in PBS buffer (pH 7.4) as shown in Fig. 2A. The LC-MS analysis clearly showed the time-dependent reduction of peptide 1-Ia (1 mM) with 2-mercaptopyridine (10 mM) in PBS (pH 7.4). We then tested the reaction rate of sulfonium tethered peptides 1-Ia and 1-Ib (1 mM) in the presence of different reductants (10 mM, 2-mercaptopyridine, thiourea or GSH) in PBS buffer (pH = 7.4) as shown in Fig. 2B and S5.† The reduction experiments were tracked by LC-MS at different time points and GSH was confirmed to be the weakest reductant among the tested reagents. The dealkylation efficiencies of different linkers and their epimers were further tested and are summarized in Fig. S6.† The peptide epimers showed briefly similar kinetics. Notably, peptide 1 equipped with linker V showed the quickest dealkylation rate (Fig. S6.†). The sulfonium center on Met is stable in 20 mM thiourea as reported by Gaunt *et al.* The on-tether sulfonium centers shown in Fig. 2B showed similar stability.²⁰ Serum stability of peptide 1 analogues was tested and the cyclic ones were found to have significantly enhanced serum stability (Fig. S7.†). To test whether our tethering strategy could improve cellular uptake, peptide 11 with three arginine residues was prepared and reactions were performed with different linkers I–VI. The reactions went smoothly with high conversions and the epimers were separated if possible. A2780 cells (Fig. 2C) and 293 T cells (Fig. S8.†) were treated with $10\ \mu\text{M}$ FAM-labeled peptides for 4 hours and then incubated with 0.05% trypan blue before FACS analysis.⁴³ In both A2780 and 293 T cell lines, the

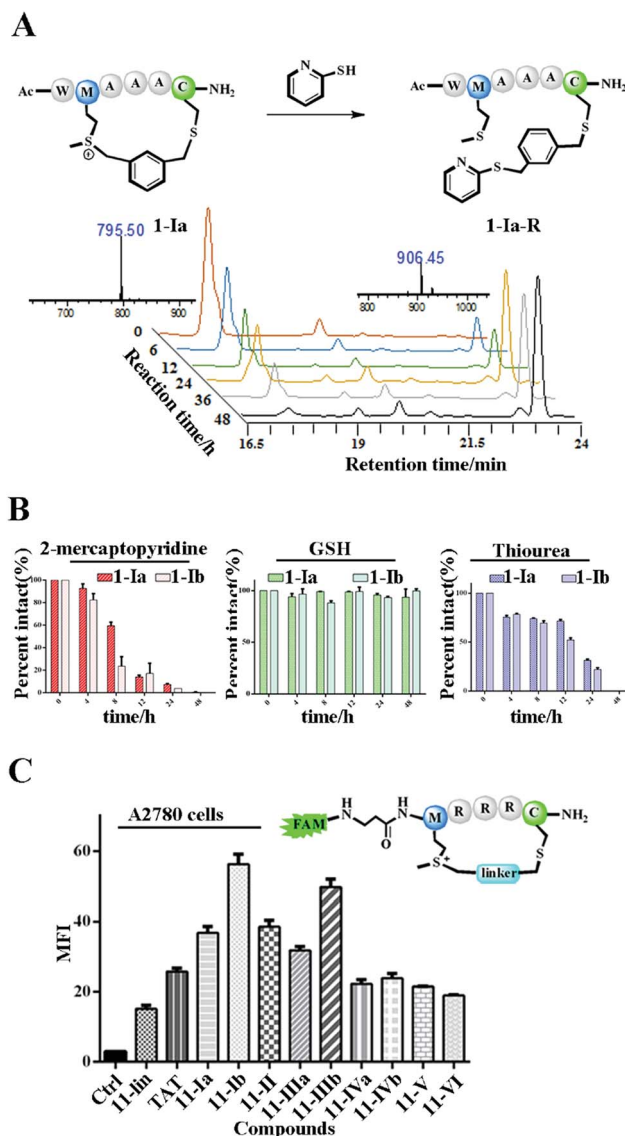


Fig. 2 The biochemical properties of the constrained peptides. (A) Dealkylation of model peptide 1-Ia (1 mM) in the presence of PyS (10 mM) in PBS (pH = 7.4) at 37°C for 48 hours. HPLC traces of the time-dependent conversion between peptide 1-Ia and its conjugated product 1-Ia-R. (B) The kinetics of peptide dealkylation reactions with different reductants under the same reaction conditions as indicated in (A). (C) Cellular uptake of the cyclic and linear peptides in A2780 cells treated with $10\ \mu\text{M}$ FAM-labeled peptides for 4 hours. All cells were incubated with 0.05% trypan blue for 3 minutes before further analysis.

constrained peptides showed significantly increased cellular uptake compared to linear peptide 11. Confocal microscopy images of A2780 cells indicated the different cellular distributions of peptides with different linkers (Fig. S9.†). To sum up, the model peptides constructed with this method showed enhanced stability and cellular uptake and could conjugate with physiologically relevant nucleophiles. Notably, the sulfonium center showed limited conjugation with GSH after 48 hours at physiologically relevant concentrations.

To further prove the potential of this methodology for proximity induced cysteine modification, we constructed



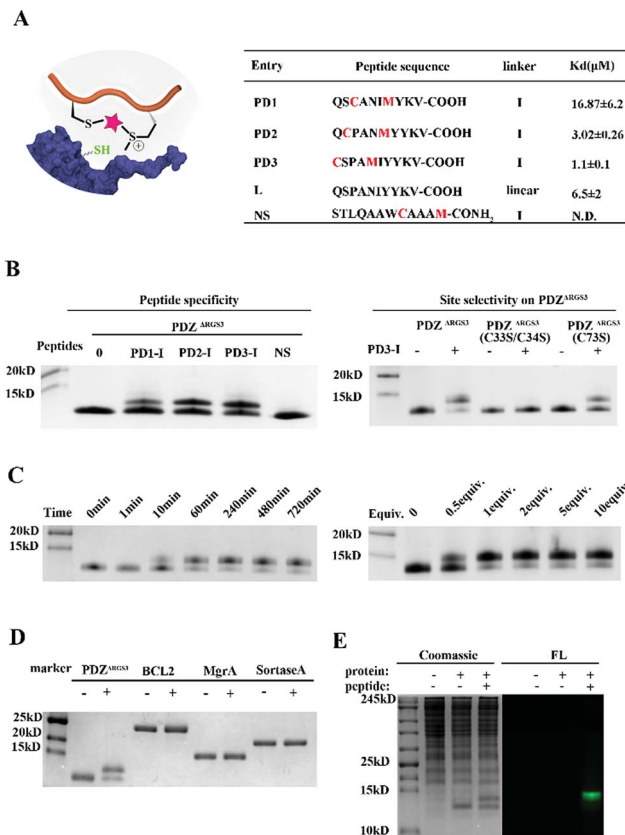


Fig. 3 Design and synthesis of reactive peptide ligands for covalent PDZ^{ARGS3} conjugation (PDZ^{ARGS3} denotes the PDZ domain of PDZ-RGS3). (A) Peptide sequences designed for protein conjugation. (B) Peptide specificity and site selective cysteine conjugation of PDZ^{ARGS3}. PDZ^{ARGS3} was reacted with different peptides (protein/peptide 20/100 μM, pH 7.4, 1 hour). PDZ mutants were incubated with peptide PD3-I (protein/peptide 20/100 μM, pH 7.4, 12 hours). (C) Reaction kinetics study of peptide PD3-I (protein/peptide 15/75 μM, pH 7.4) for 0 min, 1 min, 10 min, 60 min, 240 min, 480 min and 720 min, respectively. Stoichiometric study of peptide PD3-I from 0.5 equiv. to 10.0 equiv. by incubating with PDZ^{ARGS3} for 4 hours. (D) Ligand induced protein conjugation. Other proteins containing free Cys would not react with peptide PD3-I (protein/peptide 15/75 μM, pH 7.4, 12 hours). (E) FAM-labelled peptides (PD3-I, 50 μM) and PDZ^{ARGS3} (10 μg) were incubated with 293 T cell lysates (300 μg) for 24 hours. FL, in-gel fluorescence scanning.

peptide ligands for PDZ^{ARGS3} as shown in Fig. 3A. PDZ^{ARGS3} (PDZ^{ARGS3} denotes the PDZ domain of PDZ-RGS3, and the protein sequence is shown in Fig. S10†) plays an important role in ephrin-B reverse signaling which is associated with SDF-1 (stromal derived factor 1) neuronal chemotaxis.⁴⁴ PDZ^{ARGS3} was reported to be covalently labeled at a cysteine by a peptide ligand bearing a chloroacetamide moiety and we envisioned it as an ideal showcase for this proof-of-concept study.³⁵ There are three Cys residues (C33, C34, and C73) in the vicinity of the peptide ligand binding site of PDZ^{ARGS3}.³⁵ To study the peptide selectivity and site selective cysteine conjugation of targets, a series of peptide ligands with different cyclization sites and different PDZ^{ARGS3} mutants were then prepared including PDZ^{ARGS3} C33SC34S and PDZ^{ARGS3} C73S (Fig. 3A and S10†). We first tested the peptides' binding affinity to PDZ^{ARGS3} and their

mutants by fluorescence polarization assays shown in Fig. 3B and S11.† The peptides with different stapling sites showed quite different binding affinities, while the Cys-Ser mutations (PDZ^{ARGS3} C33S/C34S, PDZ^{ARGS3} C73S) appeared to have no obvious detrimental effects on peptide binding.

Then peptides PD1-I to PD3-I were reacted with PDZ^{ARGS3} in pH 7.4 PBS (protein/peptide 20/100 μM, 37 °C, 1 hour). As shown in Fig. 3B, peptide PD1-I with a binding affinity of 16.87 μM showed weak conjugation, while peptides PD2-I and PD3-I with a K_d of 3.02 μM and 1.1 μM showed rapid covalent conjugation. Rationally, the scrambled peptide NS with no binding affinity for PDZ^{ARGS3} couldn't conjugate with PDZ^{ARGS3}, which further confirmed the concept of ligand-induced protein conjugation. The protein conjugates still retained their secondary structure as confirmed by circular dichroism (CD) and thermal shift assays as shown in Fig. S12.† We also found that the reaction efficiency was reduced with an excess of competitive linear peptides confirming the ligand-induced conjugation (Fig. S13†). We then tested the site selectivity of peptide PD3-I with wild type PDZ^{ARGS3} and its mutants. Peptide PD3-I showed the most efficient reaction with wild PDZ^{ARGS3}, and a little weaker reaction with PDZ^{ARGS3} C73S but negligible reaction with PDZ^{ARGS3} C33SC34S (Fig. 3B). The MS data further confirmed the satisfactory covalent conjugation of PDZ^{ARGS3} C73S and poor covalent conjugation of the mutant PDZ^{ARGS3} C33SC34S (Fig. S14–S17†), indicating that the cysteine in the vicinity of the protein-peptide interaction site was essential for ligand conjugation. The reaction kinetics and stoichiometric study between PDZ^{ARGS3} and peptide PD3-I was then performed as shown in Fig. 3C. The reaction started within 10 minutes and went to an ~80% conjugation within 60 minutes. One equiv. of peptide was briefly enough to complete the conjugation. The kinetics and stoichiometric study clearly showed the efficient conjugation. We also found that the reaction efficiency was reduced in acidic buffer but went more smoothly under basic conditions (Fig. S18†). The resulting protein-peptide conjugate was stable in 10 mM GSH for at least 12 hours at 37 °C with no

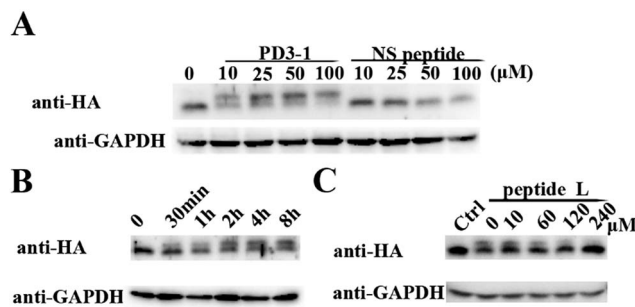


Fig. 4 The covalent reaction in HA-PDZ^{ARGS3} transfected cell lysates. (A) Covalent bonding of peptide PD3-1 or peptide NS to HA-PDZ^{ARGS3} after 8 h incubation at room temperature with HA-PDZ^{ARGS3} transfected cell lysates. (B) Reaction kinetics study of peptide PD3-1 and HA-PDZ^{ARGS3} conjugation in HA-PDZ^{ARGS3} transfected cell lysates for 0 min, 30 min, 1 h, 2 h, 4 h and 8 h respectively. (C) The high concentration of linear peptide competitively blocked the labeling of peptide PD3-1 (30 μM) to HA-PDZ^{ARGS3} in cell lysates in a dose-dependent manner.



leaks being detected (Fig. S18[†]), which hinted at its potential biological application in antibody–drug conjugates or protein post-translational modifications.

Then protein selectivity was carefully examined by using other proteins containing free Cys residues such as BCL2, MgrA and SrtA (Table S3[†]). No conjugation was observed as shown in Fig. 3D which indicates the site-selective cysteine modification of our designed peptides. To assess the ability of peptide PD3-I

to label PDZ^{ARG53} in a complex proteome environment, 293 T cell lysates (300 μg) were spiked with PDZ^{ARG53} (10 μg), and then treated with 50 μM FAM labeled peptide PD3-I as shown in Fig. 3E, referring to the work of Sun *et al.*⁴⁵ The gel data showed a clear single fluorescence band with the right molecular weight indicating a clean and selective conjugation of peptide PD3-I to PDZ^{ARG53}. The successful conjugation was further confirmed by a pull down assay using Ni-NTA agarose beads as shown in Fig. S19.[†]

The peptide was then tested for conjugation efficiency in HA-PDZ^{ARG53} transfected cell lysates as shown in Fig. 4. Anti-HA western analyses revealed that peptide PD3-I could conjugate with PDZ^{ARG53} in a concentration-dependent manner while the scrambled peptide NS couldn't label this target even at 100 μM with incubation for 8 hours, as shown in Fig. 4A. The reaction in cell lysates could be started in 30 min and reached high conjugation within 8 hours at room temperature with 50 μM PD3-I, as shown in Fig. 4B. The reaction efficiency would be decreased when competed with the excess of linear peptide ligand L, indicating that the reaction in cell lysates occurs by the ligand-induced protein conjugation (Fig. 4C). The successful conjugation in cell lysates showed its potential for future cellular applications, such as cell imaging, the study of protein–protein interaction, the discovery of covalent inhibitors and activity based protein profiling.

As different linkers demonstrated different reaction rates (Fig. S6[†]), we then tested the conjugation efficiency of peptide PD3 equipped with different linkers as shown in Fig. 5A. The linker IV showed the slowest cysteine conjugation rate. The successful conjugation was further confirmed by ESI-MS as shown in Fig. 5B, S17 and S20–S22[†] which suggested that only one cysteine residue in PDZ^{ARG53} could be conjugated with the peptide. To further identify the modification sites, trypsin digestion of a single reaction band cut from the gel was sent for MS/MS analysis as shown in Fig. 5C and S23–S25.[†] The MS/MS results suggested an expected peptide fragmentation containing both peptide PD3-I and a peptide segment containing Cys33, Cys34 or Cys73 of PDZ^{ARG53} indicating that our peptide can selectively label PDZ in the vicinity of ligand binding sites.

Conclusions

In summary, we designed a facile macrocyclization method *via* bis-alkylation between cysteine and methionine with improved serum stability and cellular uptake. Additionally, the tethered sulfonium could be a novel warhead for site selective protein modification under biocompatible conditions. To the best of our knowledge, this is the first attempt to combine peptide stapling and the installation of a selectively reacting moiety in one simple design. To demonstrate the principle, we constructed peptide ligands for PDZ^{ARG53} and clearly showed that the reaction is rapid, efficient, highly selective and solely proximity-prompted. The reaction is viable in PBS, doesn't require any further special conditions and is selective in cell lysates. This method could have great potential in affinity-based protein profiling, target identification, and novel PPI modulator development.

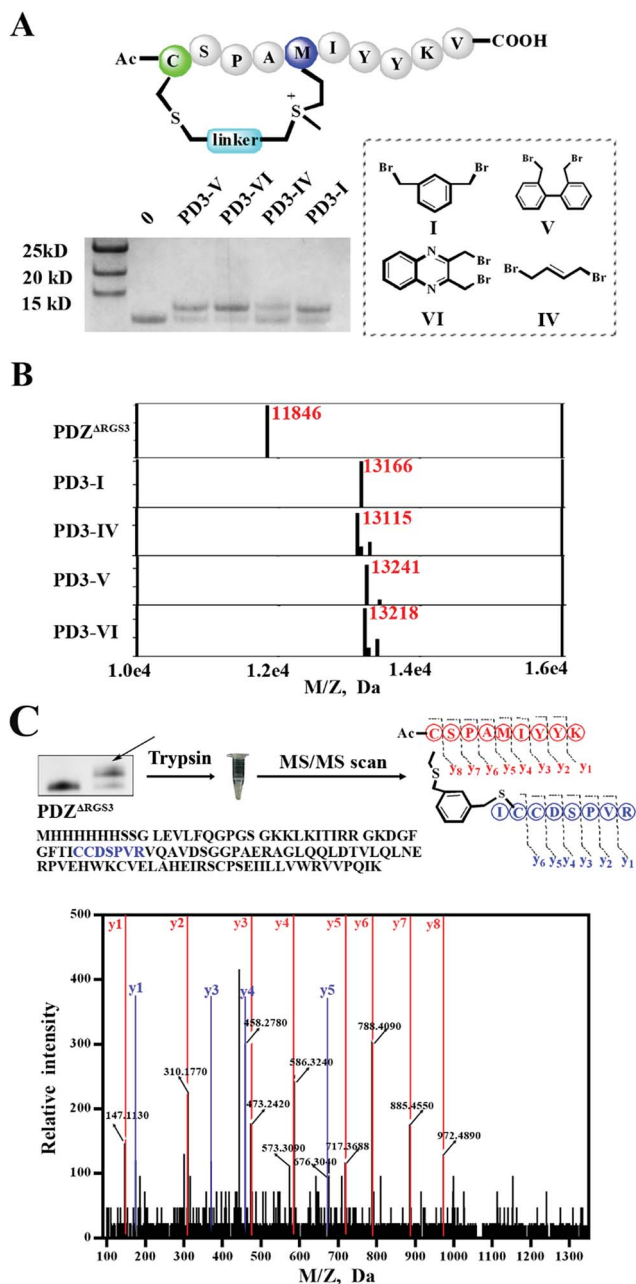


Fig. 5 ESI MS analysis of the PDZ–peptide covalent conjugates. (A) The proteins were incubated with peptides equipped with different linkers (protein/peptide 15/75 μM, pH 7.4, 12 hours). (B) The mass analysis of peptide–PDZ^{ARG53} conjugation, figures prepared using Prism based on original MS data shown in Fig. S14–S18.[†] (C) Mass/mass spectrometry analysis of trypsin-digested PDZ–peptide conjugates indicating that peptide PD3-I binds covalently to C33 or C34 in PDZ^{ARG53}.



Author contributions

Z. L., F. Y. and D. W. prepared the manuscript and designed the research presented. D. W., M. Y. and Z. H. designed and performed the synthetic and biological experiments. N. L. and C. L. prepared various proteins. R. Z. and W. L. provided HPLC, MS and CD data. R. W. and S. L. helped analyze the MS data. Y. J. and X. S. helped prepare the cellular experiments.

Conflicts of interest

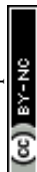
There are no conflicts of interest to declare.

Acknowledgements

We acknowledge financial support from the National Natural Science Foundation of China grants 21778009, 81701818 and 81572198; the Shenzhen Science and Technology Innovation Committee, JCYJ20170412150609690, KQJSCX20170728101942700 and JCYJ20170807144449135. This work is supported by the High-Performance Computing Platform of Peking University and Beijing National Laboratory for Molecular Sciences (BNLMS). The PDZ-RGS3 plasmid is a kind gift from Prof Jiang Xia's lab at The Chinese University of Hong Kong.

Notes and references

- R. Rakhit, R. Navarro and T. J. Wandless, *Chem. Biol.*, 2014, **21**, 1238–1252.
- N. Krall, F. P. da Cruz, O. Boutureira and G. J. Bernardes, *Nat. Chem.*, 2016, **8**, 103–113.
- E. Basle, N. Joubert and M. Pucheault, *Chem. Biol.*, 2010, **17**, 213–227.
- N. Stephanopoulos and M. B. Francis, *Nat. Chem. Biol.*, 2011, **7**, 876–884.
- C. D. Spicer and B. G. Davis, *Nat. Commun.*, 2014, **5**, 4740.
- C. Zhang, P. Dai, A. A. Vinogradov, Z. P. Gates and B. L. Pentelute, *Angew. Chem., Int. Ed.*, 2018, **57**, 6459–6463.
- A. M. Embaby, S. Schoffelen, C. Kofoed, M. Meldal and F. Diness, *Angew. Chem., Int. Ed.*, 2018, **57**, 8022–8026.
- Y. Kim, S. O. Ho, N. R. Gassman, Y. Korlann, E. V. Landorf, F. R. Collart and S. Weiss, *Bioconjugate Chem.*, 2008, **19**, 786–791.
- J. Yu, X. Yang, Y. Sun and Z. Yin, *Angew. Chem., Int. Ed.*, 2018, **57**, 11598–11602.
- S. Choi, S. Connelly, N. Reixach, I. A. Wilson and J. W. Kelly, *Nat. Chem. Biol.*, 2010, **6**, 133–139.
- J. M. Hooker, A. P. Esser-Kahn and M. B. Francis, *J. Am. Chem. Soc.*, 2006, **128**, 15558–15559.
- Y. Takaoka, H. Tsutsumi, N. Kasagi, E. Nakata and I. Hamachi, *J. Am. Chem. Soc.*, 2006, **128**, 3273–3280.
- J. C. Gildersleeve, O. Oyelaran, J. T. Simpson and B. Allred, *Bioconjugate Chem.*, 2008, **19**, 1485–1490.
- M. J. Matos, B. L. Oliveira, N. Martinez-Saez, A. Guerreiro, P. M. S. D. Cal, J. Bertoldo, M. Maneiro, E. Perkins, J. Howard, M. J. Deery, J. M. Chalker, F. Corzana, G. Jimenez-Oses and G. J. L. Bernardes, *J. Am. Chem. Soc.*, 2018, **140**, 4004–4017.
- S. R. Adusumalli, T. G. Rawale, U. Singh, P. Tripathi, R. Paul, N. Kalra, R. K. Mishra, S. Shukla and V. Rai, *J. Am. Chem. Soc.*, 2018, **140**, 15114–15123.
- S. D. Tilley and M. B. Francis, *J. Am. Chem. Soc.*, 2006, **128**, 1080–1081.
- J. M. Antos, J. M. McFarland, A. T. Iavarone and M. B. Francis, *J. Am. Chem. Soc.*, 2009, **131**, 6301–6308.
- T. Oya, N. Hattori, Y. Mizuno, S. Miyata, S. Maeda, T. Osawa and K. Uchida, *J. Biol. Chem.*, 1999, **274**, 18492–18502.
- S. Lin, X. Yang, S. Jia, A. M. Weeks, M. Hornsby, P. S. Lee, R. V. Nichiporuk, A. T. Iavarone, J. A. Wells, F. D. Toste and C. J. Chang, *Science*, 2017, **355**, 597–602.
- M. T. Taylor, J. E. Nelson, M. G. Suero and M. J. Gaunt, *Nature*, 2018, **562**, 563–568.
- T. A. Cropp and P. G. Schultz, *Trends Genet.*, 2004, **20**, 625–630.
- E. M. Sletten and C. R. Bertozzi, *Angew. Chem., Int. Ed.*, 2009, **48**, 6974–6998.
- J. M. Chalker, G. J. Bernardes and B. G. Davis, *Acc. Chem. Res.*, 2011, **44**, 730–741.
- J. M. Gilmore, R. A. Scheck, A. P. Esser-Kahn, N. S. Joshi and M. B. Francis, *Angew. Chem., Int. Ed.*, 2006, **45**, 5307–5311.
- A. J. Chmura, M. S. Orton and C. F. Meares, *Proc. Natl. Acad. Sci. U. S. A.*, 2001, **98**, 8480–8484.
- H. Nonaka, S. Tsukiji, A. Ojida and I. Hamachi, *J. Am. Chem. Soc.*, 2007, **129**, 15777–15779.
- H. Nonaka, S. H. Fujishima, S. H. Uchinomiya, A. Ojida and I. Hamachi, *J. Am. Chem. Soc.*, 2010, **132**, 9301–9309.
- B. Zakeri, J. O. Fierer, E. Celik, E. C. Chittock, U. Schwarz-Linek, V. T. Moy and M. Howarth, *Proc. Natl. Acad. Sci. U. S. A.*, 2012, **109**, E690–E697.
- Y. Liu, M. P. Patricelli and B. F. Cravatt, *Proc. Natl. Acad. Sci. U. S. A.*, 1999, **96**, 14694–14699.
- P. V. Robinson, G. de Almeida-Escobedo, A. E. de Groot, J. L. McKechnie and C. R. Bertozzi, *J. Am. Chem. Soc.*, 2015, **137**, 10452–10455.
- J. C. Henise and J. Taunton, *J. Med. Chem.*, 2011, **54**, 4133–4146.
- E. D. Deeks and G. M. Keating, *Drugs Ther. Perspect.*, 2018, **34**, 89–98.
- J. R. Brown, *Current Hematologic Malignancy Reports*, 2013, **8**, 1–6.
- A. O. Walter, R. T. Sjin, H. J. Haringsma, K. Ohashi, J. Sun, K. Lee, A. Dubrovskiy, M. Labenski, Z. Zhu, Z. Wang, M. Sheets, T. St Martin, R. Karp, D. van Kalken, P. Chaturvedi, D. Niu, M. Nacht, R. C. Petter, W. Westlin, K. Lin, S. Jaw-Tsai, M. Raponi, T. Van Dyke, J. Etter, Z. Weaver, W. Pao, J. Singh, A. D. Simmons, T. C. Harding and A. Allen, *Cancer Discovery*, 2013, **3**, 1404–1415.
- Y. Yu, M. Liu, T. T. Ng, F. Huang, Y. Nie, R. Wang, Z. P. Yao, Z. Li and J. Xia, *ACS Chem. Biol.*, 2016, **11**, 149–158.
- A. D. de Araujo, J. Lim, A. C. Good, R. T. Skerlj and D. P. Fairlie, *ACS Med. Chem. Lett.*, 2017, **8**, 22–26.
- A. J. Huhn, R. M. Guerra, E. P. Harvey, G. H. Bird and L. D. Walensky, *Cell Chem. Biol.*, 2016, **23**, 1123–1134.



- 38 A. D. de Araujo, J. Lim, K. C. Wu, Y. Xiang, A. C. Good, R. Skerlj and D. P. Fairlie, *J. Med. Chem.*, 2018, **61**, 2962–2972.
- 39 C. Hoppmann and L. Wang, *Chem. Commun.*, 2016, **52**, 5140–5143.
- 40 J. R. Kramer and T. J. Deming, *Chem. Commun.*, 2013, **49**, 5144–5146.
- 41 X. Shi, R. Zhao, Y. Jiang, H. Zhao, Y. Tian, J. Li, W. Qin, F. Yin and Z. Li, *Chem. Sci.*, 2018, **9**, 3227–3232.
- 42 J. R. Kramer and T. J. Deming, *Chem. Commun.*, 2013, **49**, 5144–5146.
- 43 Y. Tian, J. Li, H. Zhao, X. Zeng, D. Wang, Q. Liu, X. Niu, X. Huang, N. Xu and Z. Li, *Chem. Sci.*, 2016, **7**, 3325–3330.
- 44 Q. Lu, E. E. Sun, R. S. Klein and J. G. Flanagan, *Cell*, 2001, **105**, 69–79.
- 45 Y. Xie, J. Ge, H. Lei, B. Peng, H. Zhang, D. Wang, S. Pan, G. Chen, L. Chen, Y. Wang, Q. Hao, S. Q. Yao and H. Sun, *J. Am. Chem. Soc.*, 2016, **138**, 15596–15604.

